X-ray microanalytical studies of initial mineralization in induced heterotopic bone formation in guinea pigs

ANNE CHRISTINE JOHANNESSEN, RUNE NILSEN & GISLE BANG

Department of Oral Pathology and Forensic Odontology, School of Dentistry, University of Bergen, Haukeland Hospital, Norway

Johannessen, A.C., Nilsen, R. & Bang, G. X-ray microanalytical studies of initial mineralization in heterotopic bone formation in guinea pigs. *Acta Odontol. Scand.* 1981, 39, 217 – 226

Allogenic demineralized dentin implanted in the abdominal wall of quinea pigs induced heterotopic osteoid and bone formation. Samples of this tissue were frozen at – 140°C, freeze-dried at -80° C, infiltrated with Spurr® epoxy resin and polymerized. The sections were then studied in the scanning transmission electron microscope, and analytical studies were performed by means of energy dispersive microanalysis.

Osteoblasts and young osteoid osteocytes contained more calcium than undifferentiated cells and mature osteocytes. The Ca/P ratio in the cytoplasm of these young matrixproducing cells was high. Phosphorus was found in the nuclei of all cells and to a lesser extent also in the cytoplasm of cells rich in calcium. The initial extra-cellular mineral accumulation also showed a high Ca/P ratio. Small electrondense areas in these regions exhibited an amount of calcium and a Ca/P ratio resembling those of mature mineralized bone. The intial event of the mineralization process seemed to be an accumulation of calcium first in the young matrix-producing cells and then in the surrounding osteoid matrix.

The results suggested that the matrix-producing cells are actively involved in the accumulation of calcium and phosphorus both intra- and extra-cellularly.

Key-words: Bone mineralization; energy dispersive microanalysis; calcium; osteoblasts

Anne Christine Johannessen, Department of Oral Pathology and Forensic Odontology, School of Dentistry, University of Bergen, 5016-Haukeland Hospital, Norway

Mineralization of bone has previously been regarded as an extra-cellular process (16, 34), while a cellular control mechanism has been suggested lately (3, 9). Several authors have found evidence of intra-cellular binding of calcium in mineralizing hard tissues (5, 18, 19), and it has been suggested that matrix-producing cells are involved in passing minerals to the matrix (4, 11, 40). This cellular activity in the mineralizing process has been closely connected with the function of matrix vesicles which are found in mineralizing tissues (2, 3, 10). These membrane bound vesicles seem to be derived from cells involved in the hard tissue formation (30, 35, 36). Crystal-like particles have been found inside such vesicles and may be the first evidence of crystal formation in the mineralization process (3, 10). Alterations in matrix

Received for publication, February 3, 1981

components could, however, also explain the early extra-cellular and extra-vesicular mineralization and crystal formation in the initial phase of mineralization of hard tissues (8, 9, 33).

X-ray microanalysis (XMA) combining electron microscopy and energy dispersive x-ray analysis has become a new useful method for elemental analysis of diffusible as well as bound elements in biological material (13, 16). Scanning transmission electron microscopy (STEM) together with XMA of elements in thin sections of biological material after careful freezing and freeze-drying should exclude artefacts due to fixation. XMA has been applicated to a wide field of biological tissues and should be suitable for microanalysis of the mineralization process (29).

Implantation of demineralized dentin in the abdominal muscles of guinea pigs and rats has been shown consistently to induce heterotopic osteoid, bone and cartilage formation, as well as resulting in remineralization of implanted dentin (6, 7, 30). In this experimental model the bone is formed *de novo* (7, 37), and areas with various levels of mineralization are found within the same section. Recently it has been shown by transmission electron microscopy that the first mineral crystals in heterotopic bone formation are found mostly extra-cellularly, although a few crystals appeared inside matrix vesicles (31). The present study was undertaken to use the advantages of this model to investigate, by means of XMA, the accumulation of calcium and phosphorus in osteoblasts and osteocytes as well as in the surrounding matrix during the inital phase of mineralization of heterotopic bone formation.

MATERIAL AND METHODS

Thirty randomly bred male albino and pigmented quinea pigs were used and divided in three equal groups. They were fed a standard mixed diet (Norwegian standard for guinea pigs and rabbits, Statens Institutt for Folkehelse, Oslo, Norway) supplement with swedes and hay, and were given water ad *libitum*. The animals were weighed before the operation (about 500 g) and at the point of being sacrificed. Dentin was obtained from adult male guinea pigs, demineralized in HCI, freeze-dried and sterilized before the operation (7).

Four specimens of demineralized dentin were implanted in the abdominal muscles of each guinea pig. The operation was carried out under gen-

Fig. 1. A. Semi-thin section of frozen, freeze-dried and Spurr® embedded material showing an osteoblast region (obl) and undifferentiated connective tissue lying outside the osteoblasts. Toluidine blue. X 480.
B. STEM image of an osteoblast in the region (obl) shown in A. Point of analysis in the nucleus (1) and the cytoplasm (2). Analysis of the mineralizing osteoid with electron-dense area (3) and the surrounding less electron-dense zone (4). Uncoated, 100 nm sectionthickness. X 15,000
Energy spectra from spots corresponding to the numbers and arrows on B. Spot-size 125 nm. Mangification 5000 X. Counting time 100 sec.
B, 1. X-ray spectrum showing well defined signals from the nucleus representing phosphorus (P), and only small amounts of calcium (Ca). Peaks for sodium (Na), silicium (Si) and chlorine (C1) are due to radiation from external factors such as for instance Si from the instrument and Na and C1 from the embedding medium. VS: 128.
B, 2. X-ray spectrum from an anlysis of the cytoplasm showing a distinct K peak for Ca. The counts for P is lower than in the nucleus. VS: 128.
B, 3. X-ray spectrum from the electron-dense nodule. Note the reduced vertical scale (V.S.) compared to B 1, 2 and 4, and the lower Ca/P ratio (approx. 2) than in B, 4. VS: 2.
B, 4. X-ray spectrum from the less electron-dense area of the osteoid with lower Kα peak for Ca and P, but higher Ca/P ratio (approx. 5) than in the electrondense nodules (B, 3). Note the reduced vertical scale compared to B, 1 and 2. VS: 256.

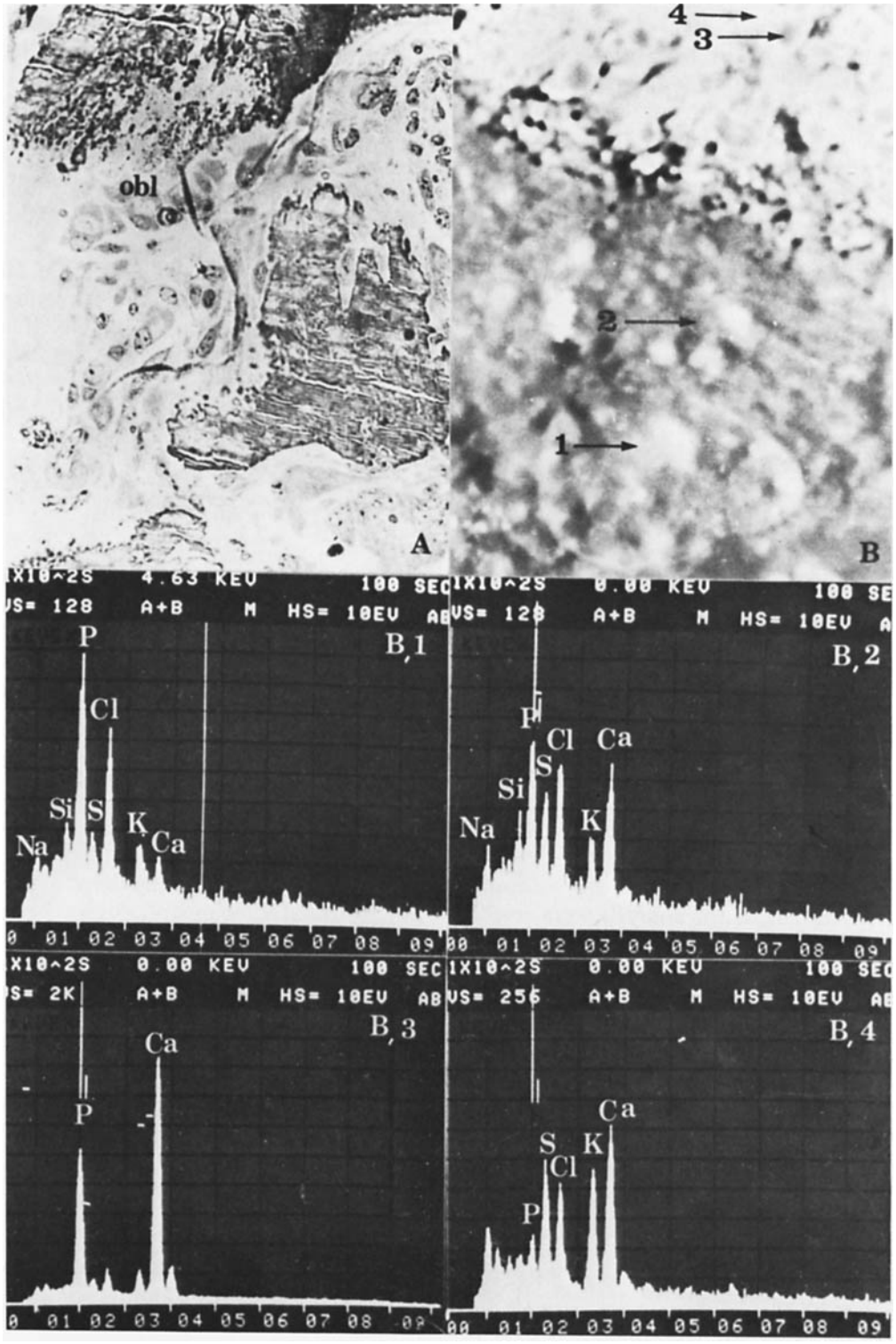
obl
A
4
3
2
1
B
B,1
P
Cl
Si
S
K
Ca
Na
B,2
P
Cl
Ca
S
Si
Na
K
B,3
Ca
P
B,4
Ca
S
K
Cl
P

eral anesthesia (Nembutal®). After 16, 21 and 28 days, respectively, the animals were killed by an overdose of Nembutal®, and the implants were dissected together with some surrounding tissue. They were cut in small pieces of 1 mm^3 and immediately frozen in isopentane prechilled with liquid nitrogen to −140°C. The specimens were stored in liquid nitrogen until further treatment. Later the tissue was freeze-dried in Tis-U-Freeze Dryer® at −80°C for three days. The freeze-dried material was warmed to room temperature in a nitrogen atmosphere before contact with air, and then embedded in Spurr® low viscosity resin while incubating in a vacuum desiccator for three days. Sections of 1 μm were cut with glass knives and stained with toluidine blue. Sectioning for further investigation was performed on a Reichert OM U 3 ultramicrotome with a diamond knife, and a section thickness of approximately 100 nm was obtained. The sections werte floated out on the inert liquid ethylene glycol and quickly picked up on carboncoated nylon grids. The scanning transmission mode (STEM) on a Philips 500 was used in the investigation. An energy-dispersive spectrometer (Kevex®) was attached to the microscope. Sections were examined, and areas for analysis were selected using the full line scan of the STEM. During the analysis the beam was stationed on the structure of interest, and x-ray spectra were obtained showing the elemental composition in the selected spot.

The Ca: P ratio was expressed as the ratio between the area of the Kα peak of Ca and the area of the Kα peak of P minus the respective backgrounds. The vertical scale (VS) was expressed as a number (128, 256, 1K (= 1 000)), showing the inverse reduction of the vertical scale.

The microscope was operated at 50 kV, spot-size 125 nm, magnification 5 000 X, counting time 100 sec. live time. The dead time was approximately zero. The beam current was controlled by calibration on a standard polished copper specimen.

RESULTS

All the animals gained weight during the experiment. Histologically the implants showed areas of resorption and fibroblastic ingrowth as well as newly formed bone in the surrounding tissues (Fig. 1 A). Remineralization of the dentin could be seen in some areas.

A detailed description of the cellular reactions has been published previously (7, 30). The light microscope findings correlated well with the STEM picture although the freeze-dried material exhibited some morphological artefacts. It was possible to study the various zones in the same sections, and the unstained sections had enough contrast to permit microanalysis both in the nu-

Fig. 2. A. STEM picture from an uncontrasted section of 100 nm showing two osteocytes which are nearly completely surrounded by fully mineralized bone. Nucleus (1) and cytoplasm (2). One part was not fully mineralized (3) resembling the zone arround the electron-dense nodules in Fig. 1 B, 4. Electron-dense matrix (4). X 5,300.

Energy spectra from spots corresponding to the number and arrows in A. Spot-size 125 nm. Magnification. Counting time 100 sec. X 5,000

A, 1. Anlysis in the nucleus showing strong signals from P and weaker from Ca. VS: 256.

A, 2. Analysis of the cytoplasm exhibiting more Ca and less P than in the nucleus. VS: 256.

A, 3. Extra-cellular measurements in osteoid showing a high Ca content and high Ca/P ratio (approx. 6). VS: 512.

A, 4. Fully mineralized bone having a high Ca level and lower Ca/P ratio (approx. 2) than the osteoid (A, 3). Note the reduced vertical scales in A, 3 and A, 4. VS: 2K.

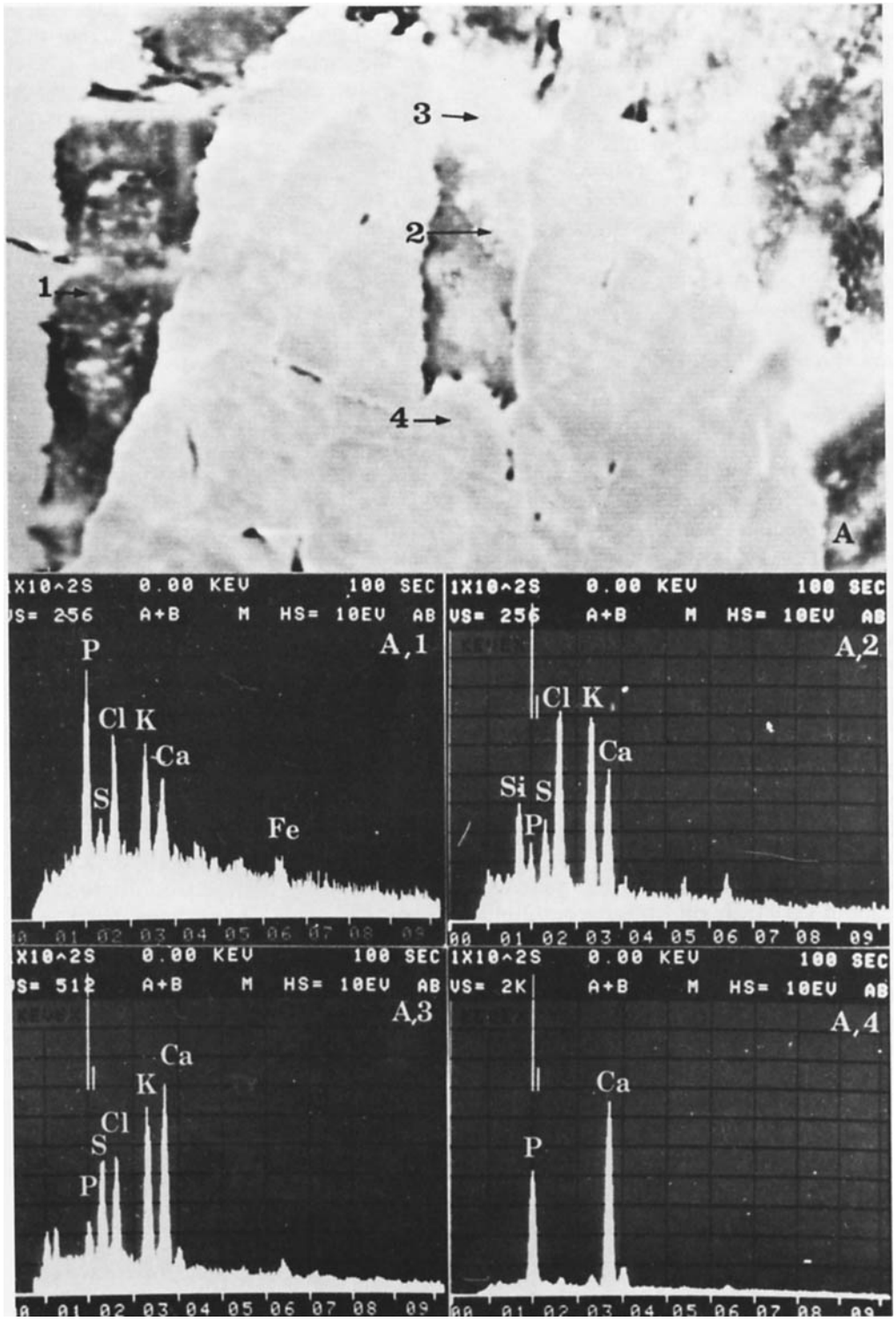
3
2
1
4
A
1X10^2S 0.00 KEV 100 SEC
VS= 256 A+B M HS= 10EV AB
A,1
P
Cl K
Ca
S
Fe
1X10^2S 0.00 KEV 100 SEC
VS= 256 A+B M HS= 10EV AB
A,2
Cl K
Ca
Si S
P
1X10^2S 0.00 KEV 100 SEC
VS= 512 A+B M HS= 10EV AB
A,3
Ca
K
Cl
S
P
1X10^2S 0.00 KEV 100 SEC
VS= 2K A+B M HS= 10EV AB
A,4
Ca
P

cleus, the cytoplasm and the extracellular matrix. Except for the nucleus the different organelles could not be recognized in the STEM, and in the undifferentiated soft tissue it was rather difficult to distinguish the cytoplasm of the cells and the extra-cellular matrix.

The different types of tissue which were found in each section permitted intra-sectional comparison between different cell types and tissue reactions. The results of microanalysis from selected cells and the surrounding matrix are shown in Figs. 1, 2 and 3.

The undifferentiated tissue showed very little calcium and phosphorus (Fig. 3 B & C), except in the nuclei which had a small peak of phosphorus Fig. 3 B). In the osteoblast region it was easier to separate extra-cellular matrix from the cytoplasm. The cytoplasm of the osteoblasts showed distinct signals from calcium (Fig. 1. B, 2). The nuclei showed distinct phosphorus peaks which were higher than in the cytoplasm, but only low counts for calcium (Fig. 1 B, 1).

The cytoplasm of the osteocytes in the osteoid (osteoid osteocytes) exhibited a high count for calcium (Fig. 2 A, 2). The nuclei showed a distinct K-peak for phosphorus (Fig. 2 A, 1). The newly formed matrix had a clear Kα peak for Ca, but very little phosphorus resulting in a Ca/P ratio of about 6:1 (Fig. 1 B, 4 and Fig. 2 A, 3). Small electron-dense nodules were also seen in the osteoid matrix (Fig. 1 B). It seemed that they increased in number and size in areas showing more mineralization. In these nodules the amount of Ca (Fig. 1 B, 3) was approximately 3 times higher than in the surrounding matrix (Fig. 1 B, 4). An increased level of phosphorus was found, resulting in Ca/P ratio of approximately 2:1 which was almost equal to that of fully mineralized bone (Fig. 2 A, 4).

The cytoplasm of the osteocytes in the fully mineralized bone had only very small Kα peaks for calcium (Fig. 3 A, 2) and negligible counts for phosphorus except in the nucleus (Fig. 3 A, 1).

Microanalysis of the remineralized dentin gave data resembling that for fully mineralized bone. Sections containing only the embedding medium showed only a distinct peak of Cl indicating that the background noise was low.

DISCUSSION

Calcium has previously been demonstrated intra-cellularly in hard tissue forming cells by several methods. Both autoradiography (15, 25) and methods utilizing calcium binding dyes such as glyoxal-bis (2-hydroxanil) at the light microscopical level (18, 19) or K-pyroantimonate at the electron microscopic level (4, 5, 12) have been used. The K-pyroantimonate method gives good ultrastructural morphology (5, 20) in contrast to the application of unfixed frozen sections used in our studies. Since the K-pyroantimonate involves fixation by OsO_4, dehydration in alco-

Fig. 3. A. The STEM image of an osteocyte in fully mineralized induced heterotopic bone. Section thickness 100 nm, uncoated. Frozen, freeze-dried and Spurr® embedded material. Uncontrasted X 9,500. The energy spectra using 125 nm spot-size (X 5,000) and counting time 100 sec. showed:
A, 1. Analysis in the nucleus with a distinct Kα-peak for P but a low peak for Ca. VS: 128.
A, 2. Analysis in the cytoplasm showed only small Kα-peak for Ca and P. VS: 128.
B. X-ray spectrum from the nucleus of a cell in undifferentiated connective tissue. 125 nm spotsize. VS: 128.
C. X-ray spectrum from the cytoplasm of the same cell as in B having no detectable Ca or P. 125 nm spot-size. VS: 128.

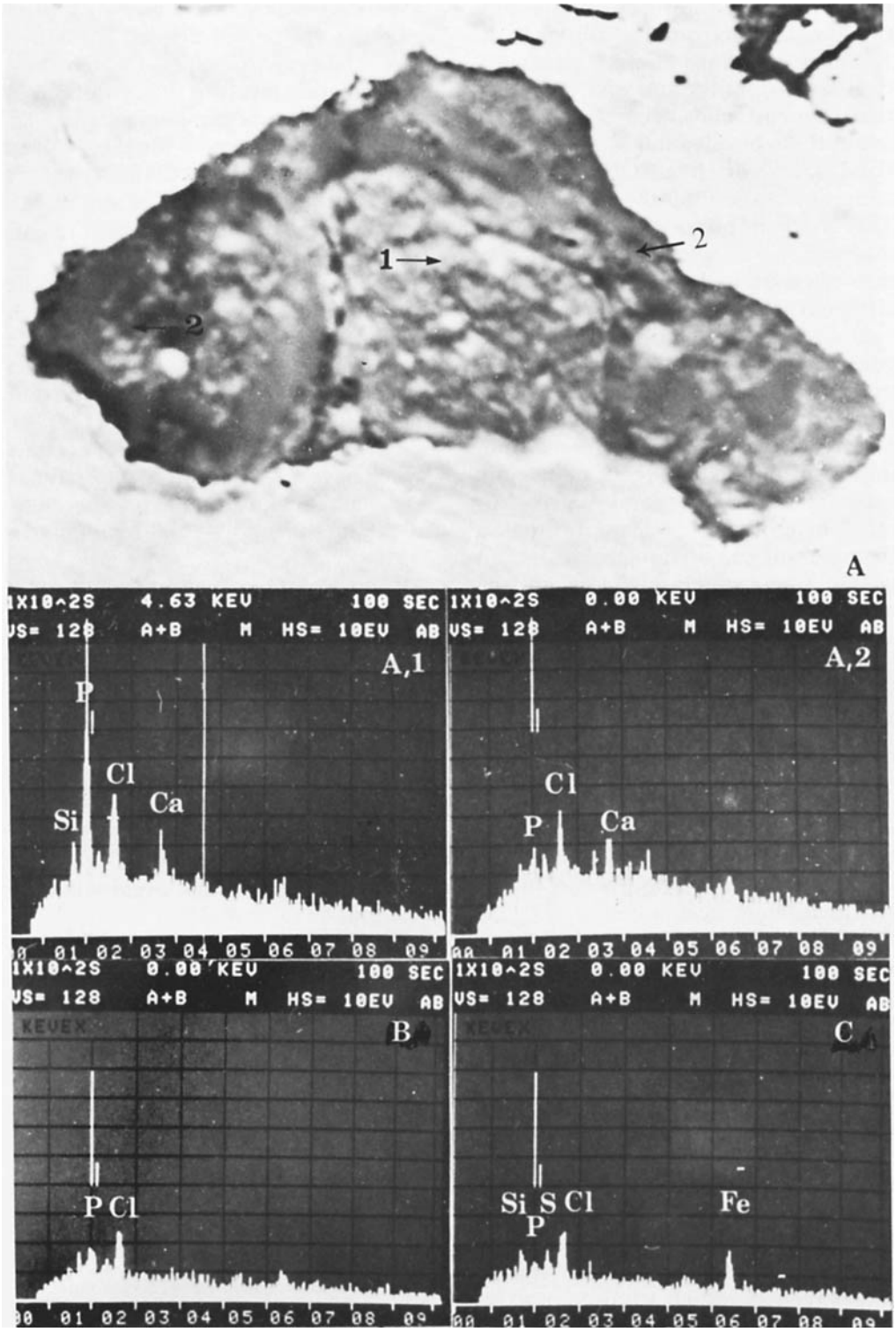
1
2
2
A
1X10^2S 4.63 KEV 100 SEC
VS= 128 A+B M HS= 10EV AB
A,1
P
Cl
Si
Ca
00 01 02 03 04 05 06 07 08 09
1X10^2S 0.00 KEV 100 SEC
VS= 128 A+B M HS= 10EV AB
A,2
Cl
P
Ca
00 01 02 03 04 05 06 07 08 09
1X10^2S 0.00 KEV 100 SEC
VS= 128 A+B M HS= 10EV AB
KEVEX
B
P Cl
00 01 02 03 04 05 06 07 08 09
1X10^2S 0.00 KEV 100 SEC
VS= 128 A+B M HS= 10EV AB
KEVEX
C
Si S Cl
P
Fe
00 01 02 03 04 05 06 07 08 09

hols and routine infiltration in epoxy, the signals from osmium will mask the Kα peaks of phosphorus, and significant redistribution and loss of the actual elements may occur (14, 21). To avoid these disadvantages we used unfixed freeze-dried material and vacuum-infiltration of the epoxy resin. This method provided a satisfactory morphology to allow performance of microanalysis in the cytoplasm and nucleus of the actual cells.

Until about 1970 mineralization was considered mainly an extra-cellular process, although Watt, as early as 1928 (40), proposed that the minerals were secreted from cells. The present findings regarding the sequence of calcium accumulation in cells and matrix during heterotopic bone formation strongly suggest that osteoblasts and young osteocytes are active in the mineralization process.

Unfixed and unstained tissue, with its low contrast and resolution, made identification of other organelles than the nucleus difficult, thus making it impossible to relate the observed cytoplasmic Ca-accumulation to the proper organelles. However, other studies using ordinary electron microscopy or the K-pyroantimonate method have suggested that mitochondriae are involved in calcium accumulation (11, 22, 23). Electrondense granules which have been found in mitochondria are interpreted as being the site of calcium accumulation, but they could possibly also be the result of cell injury (12). How the calcium is transported out of the cells is not fully understood, although it has been suggested that calcium may be bound to organic components such as collagen precursors (4), phosphoproteins (39), glycoproteins (13) or lipids (41), and subsequently secreted into the intercellular space. Matrix vesicles, which are also found in the mineralizing area of this model (32), may be involved in transport of minerals prior to crystal formation (29). The present results – which show high calcium levels in the cytoplasm of the young matrix producing cells – favour such a transport function of the matrix vesicles rather than the theory that matrix vesicles are the site of calcium accumulation as proposed in cartillage (1).

The high Ca/P ratio observed in the osteoid and lower ratio, and even higher total amounts of minerals in the electrondense nodules, may suggest that phosphatases could be involved in increasing the phosphoruslevel (24, 29).

Formation of hydroxypatite crystals which have a Ca/P ratio of approximately 2 may then be due to an alteration of the matrix into a calcifiable matrix (33, 38).

The present study indicated that the intial events in mineralization are found intra-cellularly with an increased level of calcium. Later calcium could also be demonstrated in the matrix of the newly formed osteoid. Then the total amount of calcium and especially phosphorus increased, and electron-dense nodules appeared in the tissue, possibly reflecting extensive crystal formation. Although the cells showed distinct mineral accumulation, it cannot be excluded that calcium and phosphorus may also pass outside the cells to the sites of initial crystal formation. Such a possibility has been supported in studies of dentin formation (27, 28). Based on the present results it may be concluded that young matrix-producing cells are involved in mineral accumulation in the initial mineralization during heterotopic bone formation.

Acknowledgements. The technical assistance of Turid Davidsen is highly appreciated.

We are also grateful to engineer J. Röli and prosektor H. Dalen for valuable help during this study.

This study was supported by grants from The Norwegian Research Council for Science and the Humanities (grant no. C 51.34-3).

REFERENCES

1. Ali, S.Y., Wisby, A., Evans, L. & Graig-Grey, J. The sequence of calcium and phosphorus accumulation by matrix vesicles. Calcif. Tiss. Res. Suppl. 1977, 22, 490 – 493
2. Anderson, H.C. Eletron microscopic studies of induced cartilage development and calcification. J. Cell. Biol. 1967, 35, 81 – 101
3. Anderson, H.C. & Reynolds, J.J. Pyrosphosphate stimulation of calcium uptake into cultured embryonic bones. Fine structure of matrix vesicles and role in calcification. Devel. Biol. 1973, 34, 211 – 227
4. Appelton, J. & Morris, D.C. An ultrastructural investigation of the role of the odontoblast in matrix calcification using the potassium pyroantimonate osmium method for calcium localization. Archs Oral. Biol. 1979, 24, 467 – 475 (a)
5. Appelton, J. & Morris, D.C. The use of potassium pyroantimonate-osmium method as a means of identifying and localizing calcium at the ultrastructural level in the cells of calcifying system. J. Histochem. Cytochem. 1979, 27, 676 – 680 (b)
6. Bang, G. & Urist, M.R. Bone induction in excavation chambers in matrix of decalcified dentin. Arch. Surg. 1967, 94, 781 – 789
7. Bang, G. Induction of heterotopic bone formation by demineralized dentin in guinea pigs: relationship to time. Acta Pathol. Microbiol. Scand. Sect. A. Suppl. 1973, 236, 60 – 70
8. Baylink, D., Wergedal, J. & Thompson, E. Loss of proteinpolysaccharides at sites where bone mineralization is initiated. J. Histochem. Cytochem. 1972, 4, 279 – 292
9. Becker, G.L. Calcification Mechanisms: Roles for cells and mineral. J. Oral Path. 1977, 6, 307 – 315
10. Bonucci, E. & Gherardi, G. Histochemical and electron microscope investigations on medullary bone. Cell. Tissue Res. 1975, 163, 81 – 97
11. Brighton, C.T. & Hunt, R.M. Histochemical localization of calcium in growth plate mitochondria and matrix vesicles. Federation Proc. 1976, 35, 143 – 147
12. Burger, E.H. & Matthews, J.L. Cellular calcium distribution in fetal bone studied with K-pyroantimonate. Calcif. Tiss. Res. 1978 26, 181 – 190
13. de Bernard, B., Stagni, N., Vittur, F. & Zanetti, M. Role of Ca. $^{2+}$ binding glycoprotein in the process of calcification. In: Wasserman, R.H. ed. Calcium-binding proteins and calcium function. North Holland; New York, Amsterdam, Oxford 1977, pp. 228 – 231
14. Echlin, P. & Saubermann, A.J. Preparation of biological specimens for x-ray microanalysis. Scanning Electron Microscopy, part I, 1977, 621 – 638
15. von Fromme, H.G., Höhling, H.J. & Riedel, Elektronmikroskopische Studien über die Dentinbildung. 1. Mitteilung: Localization von Calcium und alkalischer Phosphatase. Dtsch. zahnärztl.z. 1971, 26, 359 – 364
16. Glimcher, M.J. and Krane, S.M. The organization and structure of bone, and the mechanism of calcification. In: Gould, B.S. ed. Treatise on collagen, vol. 2. Biology of collagen, part B. Acad. Press. London and New York 1968, pp. 67 – 241
17. Hall. T.A. Biological X-ray microanalysis. J. Microsc. 1979, 117, 145 – 163
18. Kashiwa, H.K. Calcium in cells of fresh bone stained with glyoxal bis (2-hydroxyanil). Stain Technol. 1966, 41, 49 – 55
19. Kashiwa, H.K. Calcium phospate in osteogenic cells. Clin. Orthop. 1970, 70, 200 – 211
20. Klein, R.L., Yen, S.S. & Thureson-Klein, A. Critique on the K-pyroantimonate method for semiquantitative estimation of cations in conjuction with electron microscopy. J. Histochem. Cytochem. 1972, 20, 65 – 78
21. Landis, W.J., Paine, M.C. & Glimcher, M.J. Electronmicroscopic observations of bone tissue prepared anhydrously in organic solvents. J. Ultrastruct. Res. 1977, 59, 1 – 30
22. Lehninger, A.L. Mitochondria and calcium ion transport. Biochem. J. 1970, 119, 129 – 138
23. Lehninger, A.L., Reynafarje, B., Vercesi, A. & Tew, W.P. Transport and accumulation of calcium in mitochondria. New York Acad. Sci. 1978, 307, 160 – 176
24. Magnusson, B.C. The effects of magnesium and calcium ions on phosphate activities at alkaline pH in the molar region of newborn mice. Histochem 1974, 42, 211 – 219
25. Matthews, J.L., Martin, J.H. & Collins, E.J. Metabolism of radioactive calcium by cartilage. Clin. Orthop. 1968, 58, 213 – 223
26. Morris, D.C. & Appelton, J. Ultrastructural localization of calcium in the mandibular condylar growth cartilage of the rat. Calcif. Tissue Int. 1980, 30, 27 – 34
27. Munhoz, C.O.G. & Leblond, D.P. Deposition of calcium phosphate into dentin and enamel as shown by radioautography of sections of incisor teeth following injection Ca^{45} into rats. Calc. Tiss. Res. 1974, 15, 221 – 235
28. Nagai, N. & Frank, R.M. Electron microscopic autoradiography of Ca^{45} during dentinogenesis. Cell. Tiss. Res. 1974, 155, 513 – 523
29. Nicholson, W.A.P., Ashton, B.A., Höhling, H.J., Quint, J., Scheiber, J., Ashton, I.K. &

Boyde, A. Electron microprobe investigations into the process of hard tissue formation. Cell. Tiss. Res. 1977, 177, 331 – 345
30. Nilsen, R. Electron microscopy of induced heterotopic bone formation in guinea pigs. Archs Oral. Biol. 1977, 22, 485 – 493
31. Nilsen, R. Electron microscopic study of mineralization in induced heterotopic bone formation in guinea pigs. Scand. J. Dent. Res. 1980, 88, 340 – 347
32. Nilsen, R. Microfilaments in cells associated with induced heterotopic bone formation in guinea pigs. An immunofluorescence and ultrastructural study. Acta Pathol. Microbiol. Scand. Sect. A. 1980, 88, 129 – 134
33. Nygren, H., Persliden, B., Hansson, H.-A. & Linde, A. Cathepsin D: Ultra-immunohistochemical localization in dentinogenesis. Calcif. Tissue Int. 1979, 29, 251 – 256
34. Robinson, R.A., Doty, S.B. and Cooper, R.R. Electron microscopy of mammalian bone. In: I. Zipkin ed. Biological mineralization. Wiley-Interscience N.Y., London, Sydney, Toronto 1973, pp. 261 – 265
35. Rabinovitch, A.L. & Anderson, H.C. Biogenesis of matrix vesicles in cartilage growth plates. Fed. Proc. 1976, 35, 112 – 116
36. Thyberg, J. & Friberg, U. Electronmicroscopic enzyme histochemical studies on the cellular genesis of matrix vesicles in epiphyseal plate. J. Ultrastruct. Res. 1972, 41, 43 – 59
37. Urist, M.R. Bone formation by autoinduction. Sci. 1965, 150, 893 – 899
38 Urist, M.R. Biochemistry of calcification. In: Bourne, G.H. ed. The biochemistry and physiology of bone, vol. IV. Acad. Press. New York, San Fransisco, London 1976, pp. 11 – 25
39. Veis, A., Sharkey, M. and Dickson, I. Noncollagenous proteins of bone and dentin extracellular matrix and their role in organized mineral deposition. In: Wasserman, R.H. et al. eds. Calcium-binding proteins and calcium function. pp. 409 – 418
40. Watt. J.C. The development of bone. Arch. Surg. 1928, 17, 1017 – 1046
41. Wuthier, R.E. Lipids of matrix vesicles. Fed. Proc. 1976, 35, 117 – 121